Research Square

Preprints are preliminary reports that have not undergone peer review. They should not be considered conclusive, used to inform clinical practice, or referenced by the media as validated information.

Enhancing Crop Resilience: A Deep Learning Framework for Timely Identification of Potato Leaf Diseases Through NLSCTAN and IoT Integration

Rupali Maske

rupali.mofc123@gmail.com

Sathyabama Institute of Science and Technology, Chennai, Tamil Nadu, India.

Research Article

Keywords: Potato leaf disease classification, Global response normalization, Deep learning, Fertilizer recommendation, Modified walrus optimizer

Posted Date: March 11th, 2025

DOI: https://doi.org/10.21203/rs.3.rs-6188570/v1

License: This work is licensed under a Creative Commons Attribution 4.0 International License. Read Full License

Additional Declarations: The authors declare no competing interests.

Enhancing Crop Resilience: A Deep Learning Framework for Timely Identification of Potato Leaf Diseases Through NLSCTAN and IoT Integration

[1,*]Rupali Maske, [2]B. Bharathi

[1,*] Research Scholar, Department of CSE, Sathyabama Institute of Science and Technology, Chennai, Tamil Nadu, India.

[2] Professor, Department of CSE, Sathyabama Institute of Science and Technology, Chennai, Tamil Nadu, India.

[*]Corresponding author: rupali.mofc123@gmail.com

Abstract

Potato disease management is crucial to reducing significant crop losses in agriculture. The timely identification and classification of potato leaf diseases are necessary but time-consuming and labor-intensive. Therefore, an automated model capable of accurate and timely recognition and classification is key to resolving these challenges. In this research, a novel Normalized Long-Short Convoluted Temporal Attention Network (NLSCTAN) with Internet of Things (IOT) is developed to classify infected potato leaves and provide fertilizer suggestions to combat diseases. This work introduces a diverse dataset collected from IOT sensors by merging similar classes from three distinct potato leaf datasets: the potato leaf disease dataset, potato leaf diseases, and the plant village dataset. Preprocessing is performed using adaptive Contrast-Limited Adaptive Histogram Equalization (CLAHE) with double gamma correction to enhance the image quality. Feature extraction involves extracting different texture features using ternary patterns and discrete wavelet transform. Subsequently, dimensionality reduction is achieved through an auto encoder. Finally, the NLSCTAN model combines segmentation and classification processes to extract infected regions, determine their identity, and suggest appropriate fertilizers. Modified walrus optimization further enhances accuracy by minimizing the loss function of the neural network. The proposed procedure outperforms existing models, achieving a mean accuracy of 99.2% across various potato disease types. Experimental findings validate its competitiveness and effectiveness.

Keywords: *Potato leaf disease classification, Global response normalization, Deep learning, Fertilizer recommendation, Modified walrus optimizer*

1. Introduction

"IoT for leaf detection" refers to the use of Internet of Things (IoT) technology, such as sensors and cameras, that automatically recognize the situation of leaves on plants, often with an objective of identifying diseases or stress that affect crops through evaluating visual characteristics such as color, shape, and texture, allowing for prompt treatment in a smart farming system. Agriculture plays a critical role in upholding economic strength, stability and societal welfare. With technological advances, agriculture has revolutionized farming equipment and methods through new artificial intelligence procedures like computer vision. Automatic plant disease detection has gained significant attention [1-2]. Factors like chemical misuse, climate change, pollution, and new pathogens have increased plant diseases, threatening crop production, food security, and public health. Consequently, diagnosing, analyzing, and identifying plant diseases is crucial for improving decision-making in crop disease control, invasion prevention, pesticide use, and pollution management [3-4].

Potatoes produce more starch, wet matter, amino acids, and micronutrients per unit area than cereals, resulting in higher productivity [5]. Nevertheless, diseases such as early and late blight significantly reduce potato yield, impacting the national economy and farmers' livelihoods. These blight diseases rank among the most destructive plant diseases worldwide, affecting both production and nutritional value [6-7]. Artificial intelligence model improves early detection and categorization of agricultural diseases, promoting sustainable growth. Automated diagnosis during the budding period boosts potato crop output, reducing the need for labor-intensive and time-consuming manual interpretations [8-9].

Existing approaches rely on imaging technology, from simple RGB photos to advanced systems like infrared, hyperspectral, and Light Detection And Ranging (LIDAR) models [10]. These detects diseases early by analyzing leaf reflectance at different wavelengths but need specialized lab equipment [11]. In contrast, smartphones allow easy image capture for analysis via computer vision apps, benefiting amateurs' experts, or farmers. This protocol is especially efficient for small-scale farmers in developing countries. Recent advancements from classical Machine Learning (ML) to Deep Learning (DL) have significantly increased classification decisions [12-13].

Despite initial successes, the problem remains challenging. One primary complexity in developing ML models for disease diagnosis is the requirement for large, high-quality datasets for training and testing. Another issue is dataset imbalance, which hinder achieving balanced classification. Identifying and classifying diseases with similar early symptoms is also difficult [14]. DL models often act as black boxes, lacking interpretability, making it hard to represent the most efficient features for classification. Additionally, system accuracy may be inconsistent due to factors like dataset size, imbalance, and feature selection [15]. Therefore, a more comprehensive system for accurate feature extraction and diagnosis is needed, especially for diseases with similar symptoms, to improve diagnosis efficiency and patient outcomes while reducing healthcare costs. The principal contributions of this research are,

- An innovative NLSCTAN is introduced for accurate potato leaf disease classification. The proposed NLSCTAN model significantly sharpens the precision of detecting diseases by effectively leveraging Long Short Term Memory (LSTM) and attention layers for robust temporal feature learning, ensuring precise localization of disease regions through Region Proposal Networks (RPN).
- Additionally, the integration of Global Response Normalization (GRN) improves the model's generalization ability, delivering predictions that are more accurate and stable.
- In contrast to traditional models, the proposed techniques not only identify potato leaf diseases but also recommend appropriate fertilizers based on the specific disease detected. This integrated approach provides farmers with valuable insights, leading to improved agricultural productivity and crop health.
- Another important contribution of this work is the combination of all publicly available potato leaf disease datasets to create a more effective data structure for DL schemes. The largest dataset, formed by merging various sources, is divided into validation, testing, and training sets to measure the DL model's generalization abilities.

The remaining manuscript is arranged as follows: Section 2 summarizes existing potato leaf disease detection models. Section 3 presents the proposed model for potato leaf disease detection. Section 4 illustrates experiment analysis and comparative studies. Section 5 concluded the research and suggests directions for future work.

2. Literature survey

Many researchers have recently focused on potatoes, publishing various image processing procedures for disease identification. Here is a summary of a few key works.

Elshewey AM et al. (2024) [16] developed a method to enhance potato late blight classification accuracy using GoogLeNet, ResNet-50, VGG19Net, and AlexNet pre-trained models. AlexNet was used to extract features, yielding the optimum results. Features were selected by several optimization procedures, with WaterWheel Plant Algorithm Sine Cosine (WWPASC) achieving the optimum results. Five machine learning models were trained, with MLP being the most accurate. However, the method's complexity was a notable disadvantage. ***Jha P et al. (2024) [17]*** suggested an innovative technique combining DL and image processing, featuring a deep neural network ensemble of MobileNet, Inception, and residual network techniques. Trained with a broad dataset of healthy and infected potato leaves, it accurately classifies leaves into three categories. However, the model's high computational requirements are notable disadvantages. ***Xu Y et al. (2024) [18]*** developed a dual-stage model for severity grading of late and early blight in potato leaves. First, Coformer categorized potato leaves into different classes. Then, SegCoformer segments leaves, backgrounds and lesions from the images and assigned severity labels to the lesions. However, the models showed relatively insufficient adaptability and generalization performance for leaves at different growth stages. ***Gupta HK and Shah HR et al. (2023)[19]*** developed a Convolutional Neural Network (CNN) algorithm to detect leaf diseases. The suggested model involved dataset gathering, training, testing, and classification to identify diseased or healthy potato leaves, utilizing IoT and CNN for alerts. K-Nearest Neighbour (KNN) and CNN methods were compared. However, achieving higher accuracy proved challenging, and the method's complexity is a notable disadvantage. ***Arshad F et al. (2023) [20]*** presented a hybrid DL technique for predicting potato leaf diseases. Combining VGG19 and Inception-V3 models with vision transformers, the model was trained and evaluated using a public potato leaf dataset. However, training each module proved time-consuming. ***Chen J et al. (2023) [21]*** suggested a weakly-supervised learning technique for identifying potato leaf diseases using a modified MobileNet-V2 architecture. An integrated attention process with spatial and channel attention was used for high-dimensional features extraction. This approach outperformed others, achieving superior performance. Inconsistent light intensities may hinder feature extraction, resulting in misclassification of leaf diseases. ***Feng J et al. (2023) [22]*** developed the ShuffleNetV2 2× technique for quicker inference and enhanced generalization. Different strategies were utilized: adding an attention component, cutting the number of 1×1 convolutions and minimizing network depth, and. Experiments identified the best improvements. However, the model failed to detect multiple diseases simultaneously. ***Kumar A, and Patel VK (2023) [23]*** developed a Hierarchical DLCNN(HDLCNN) for leaf disease recognition. The process starts with median filtering to remove noise, followed by Intuitionistic Fuzzy Local Binary Pattern (IFLBP) for feature extraction. The HDLCNN then detects and classifies diseases, aiding farmers via decision support systems. However, the failed to analyze the model's generalization ability across diverse conditions. ***Chen W et al. (2022) [24]*** developed Mobile Octave convolution network (MobOca_Net) for potato diseases classification. In this work, MobileNet V2 was utilized as the base and enhanced its learning capability by integrating an attention mechanism and octave convolution to capture intricate high-dimensional features. However, the model's generalization ability in diverse agricultural conditions was a notable disadvantage.

Problem statement:

Many problems persist within the domain of DL methods for potato leaf disease detection. Firstly, existing methods often struggle with accurately identifying potato leaf diseases across different regions due to overreliance on training solely with the plantvillage dataset. This limitation stems from variations in potato diseases worldwide, influenced by factors like shape, size, and background. Consequently, current systems exhibit a higher false negative rate when attempting to recognize potato diseases in diverse regions. Additionally, prevalent overfitting issues hinder the ability of these models to generalize effectively across various agricultural contexts. Furthermore, these systems frequently fail to provide suitable fertilizer recommendations tailored to specific disease conditions, limiting their practical utility for farmers.

3. Proposed potato leaf disease segmentation and classification technique

Prompt detection of potato leaf diseases offers benefits like increased crop productivity, reduced chemical dependency, and stronger plant cultivation, improving economic yields. However, automated timely detection faces challenges due to varied disease manifestations and environmental factors. Existing literature suggests DL solutions, yet integrating multiple datasets could enhance the comprehensive dataset for potato leaf disease segmentation and detection. The workflow and process illustrated in Figure 1.

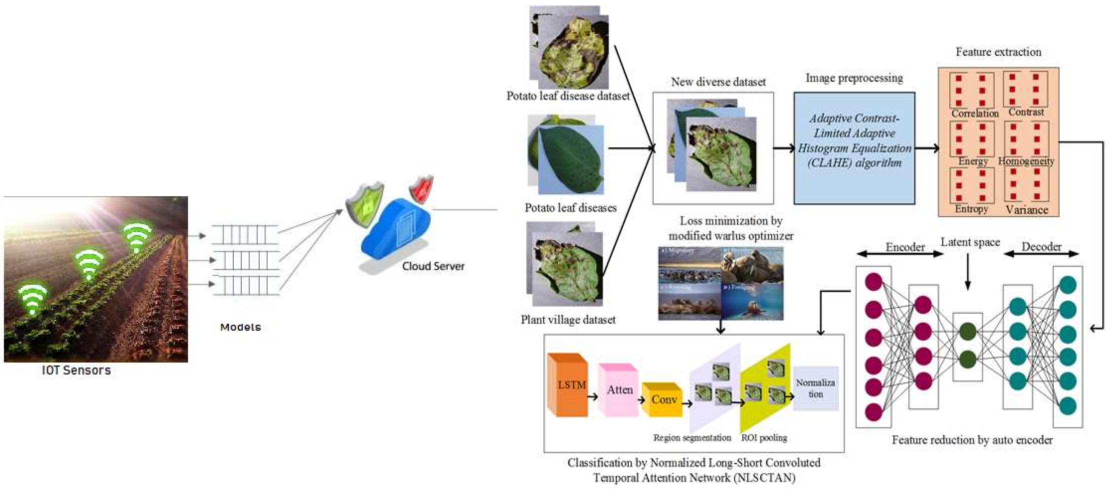

Figure 1: Work flow of the proposed methodology

Figure 1: demonstrates the proposed methodology, where the data is collected from IOT sensors deployed into the agriculture land. The sensors fetch the spatial features from the plant such as (the leaf, leaf structure, color, yield, etc.). This data is transferred to preprocessing and further segmentation and classification. This research work introduces a diverse dataset by merging similar classes from three distinct potato leaf datasets: potato leaf disease dataset, potato leaf diseases and plant village dataset. Image quality is improved by adaptive CLAHE with double gamma correction preprocessing. Feature extraction involves extracting six texture features by Ternary Patterns and Discrete Wavelet Transform (TP-DWT). Dimensionality reduction is achieved through an Auto Encoder (AE). Disease segmentation-based classification employs a NLSCTAN for improved generalization, robustness, and stability during training. Modified Walrus Optimization (MWO) further enhances accuracy by minimizing the loss function of the NLSCTAN. The process supports timely disease recognition and recommends suitable pesticides and fertilizers to increase potato crop yield.

3.1 Data collection

Deep learning models excel in learning from vast data, but their performance hinges on dataset quality and size. Precise datasets reflecting real-world scenarios offer rich learning opportunities, enabling accurate predictions. Conversely, small or biased datasets hinder generalization, leading to poor performance on new data. Large, diverse datasets not only save time and resources by serving multiple models but also drive innovation, guiding discoveries as much as the models do. However, public datasets on potato leaf diseases are limited, with only three available: 3-class potato leaf disease dataset, 3-class potato leaf diseases, and the 38-class plant village dataset. This research work combined similar disease classes from these datasets to create a larger, more effective dataset for DL algorithms. After the data collection process, preprocessing is performed to enhance image quality.

3.2 Preprocessing by adaptive Contrast-Limited Adaptive Histogram Equalization (CLAHE) algorithm

The traditional CLAHE performs well in contrast improvement but faces limitations with strong shadows in dark images. Higher clip points are needed for non-uniform blocks to enhance texture and details effectively. However, it lacks robustness in maintaining image tone, necessitating adaptive clip point setting. This research work proposes automated CLAHE [25] for image contrast improvement, utilizing gamma correction and adaptively setting clip points based on content.

Initially, the image is broken into identical rectangular blocks, and histogram equalization is applied within each block. Block texture is evaluated using average standard deviation and gray value. Higher dynamic range blocks receive higher clip points adaptively using Equation (1),

$$\beta = \frac{A}{B}\left(1 + G\frac{B_{\max}}{H} + \frac{\alpha}{100}\left(\frac{\sigma}{mean + c}\right)\right) \tag{1}$$

where, A indicates the total pixels in every bock, and the dynamic range of these blocks are represented by B. G and α denote the parameters controlling weights for dynamic range and entropy terms. $mean$ and σ signifies the block's mean and standard deviation, respectively. c denotes the small value to prevent division by 0. H denotes the full dynamic range of the image and $B_{\max}$ indicates the highest value in the block.

When pixel values undergo gamma correction, a fixed parameter causes uniform changes across regions, leading to contrast distortions. Therefore, double gamma correction is utilized within the CLAHE framework to address these distortions. A weight improvement for global gray levels of blocks using gamma correction γ_1 is defined by Equation (2):

$$\omega_{en} = \left(\frac{L_{\max}}{L_{\alpha}} \right)^{1-\gamma_1} \tag{2}$$

where ω_{en} refers to the weighting function, $L_{\max}$ denotes the maximum image's gray value, and reference grey value is denoted by L_{α}.

The output function $T_1(B)$ after first gamma correction is employed by Equation (3),

$$T_1(B) = B'_{\max} \times cdf(B) \tag{3}$$

where $B'_{\max}$ refers to the enhanced maximum grey level value in the block, and $cdf\ (B)$ represents the cumulative density function of the grey levels in the block. When an image contains both very dark and bright regions, dark regions may be under-enhanced. The γ_1 mapping curve-based CLAHE enhances contrast uniformly across the image, regardless of content. To address this, a second gamma correction is performed for contrast improvement. The subsequent gamma correction γ_2 , adjusts contrast with the final mapping function $(T\ (B))$, as represented in Equation (4),

$$T(B) = \begin{cases} Max\left(T_1(B), Gamma(B)\right) & if\ \ r > D_{threshold} \\ Gamma(B), & else \end{cases} \tag{4}$$

where $Gamma\ \ (B)$ indicates the second gamma correction process, r refers to the dynamic range of the image block, and $D_{threshold}$ indicates a predefined threshold to decide whether to apply the dual gamma correction. After preprocessing, the TP-DWT technique is applied to perform texture feature extraction.

3.3 Ternary Patterns and Discrete Wavelet Transform (TP-DWT) for texture feature extraction

The developed TP-DWT [26] combines Ternary Pattern (TP), Discrete Wavelet Transform (DWT), and a texture feature extraction function. Multilevel feature extraction networks are intricate, whereas TP-DWT utilizes lightweight, cognitive algorithms effectively. TP, DWT, and texture extraction are potent for image processing. To resolve TP's threshold value challenge, a multiple threshold approach based on standard deviation is employed. The mathematical formulation is described in Equation (5),

$$Threshold_S = SD(\mathrm{Im}\,age) \times \frac{S}{10}, \quad S = \{1,2,3,.....10\} \tag{5}$$

where $Threshold$ indicates the threshold values, SD denotes the standard deviation and S denotes the multiplication function. A texture feature extraction process is applied to extract features from lower and upper ternary histograms, containing six texture features (correlation, contrast, energy, homogeneity, entropy, variance) of leaf images [27]. The mathematical formulations of these features are given in Equations (6-11),

$$Energy = \sum_{p,q=0}^{M-1} D(p,q)^2 \tag{6}$$

$$Contrast = \sum_{p,q=0}^{M-1} (p,q)^2 D(p,q) \tag{7}$$

$$Correletio\ n = \sum_{p}^{M-1} \sum_{q}^{M-1} (pq) D(p,q) - \mu_m \mu_n / \sigma_m \sigma_n \tag{8}$$

$$Homogeneit\ y = \sum_{p,q=0}^{M-1} D(p,q) / \left(1 + (p,q)^2\right) \tag{9}$$

$$Entropy = \sum_{p,q=0}^{M-1} D(p,q) \log\ D(p,q) \tag{10}$$

$$Variance = \sum_{p}^{M-1} \sum_{q}^{M-1} (p-\mu)^2 D(p,q) \tag{11}$$

In Equation (6-11), p,q denotes the pixel values in the images, M specifies the number of different grey levels in the image and $D(p,q)$ represents the frequency of pixel pairs p,q. μ_m and μ_n denote the mean of the row and columns of the matrix. σ_m and σ_n indicate the standard deviation of the wow and columns of the matrix. μ denotes the mean grey value. After feature extraction, the extracted features are given to AE technique for dimensionality reduction process.

3.4 Dimensionality reduction by Auto Encoder (AE) model

An AE is an unsupervised neural network that learns to reconstruct input data by reducing its dimensionality. It approximates the identity function, resulting in the output closely matching the input but with fewer dimensions.

Consider $Y_1, Y_2, \ldots Y_M \in \Re^N$ represents M data points and Y denotes a data matrix with rows $Y_1, Y_2, \ldots\ldots Y_M$. Assume Y is normalized (Column means centered at zero, with standard deviations normalized to one) [28]. The simple AE encodes input $Y_m \in \Re^N$ into a hidden representation (I_m) , as represented in Equation (12),

$$I_m = \sigma(Y_m \omega + \mathrm{B}), m = 1,2,\ldots..N \tag{12}$$

In Equation (12), N denotes the number of input neurons, ω indicates the weight matrix, σ represents the activation function and B represents a bias vector. The hidden layer compresses input data into encoded, latent, or low-dimensional space. Then, the hidden representation is decoded to reconstruct $\hat{Y}_m$, denoted in Equation (13),

$$\hat{Y}_m = \sigma'(I_m \omega' + \mathrm{B}') \tag{13}$$

where ω' refers to the another weight matrix, σ' specifies the another activation function, and B' indicates the another bias vector. Finally, the AE is trained to decrease the mean squared error using Equation (14),

$$\underset{\omega,\omega',\mathrm{B},\mathrm{B}'}{Minimize} \frac{1}{M} \sum_{m=1}^{M} \sum_{n=1}^{N} \left(\hat{Y}_{mn} - Y_{mn} \right)^2 \tag{14}$$

In Equation(14), M indicates the total number of data points, $\hat{Y}_{mn}$ and Y_{mn} represent the reconstructed and original values of the n^{th} feature for the m^{th} data points. The reduced feature dimensions are fed into a NLSCTAN with the Modified Walrus Optimization (MWO) algorithm for segmentation-based classification.

3.5 Classification by Normalized Long-Short Convoluted Temporal Attention Network (NLSCTAN) with the Modified Walrus Optimization (MWO) algorithm

In the DL-based leaf disease segmentation and classification technique, a NLSCTAN model effectively segments and classifies leaves. First, LSTM and attention layers learn temporal dependencies among features. The attention block helps the network focus on disease-affected areas, suppress irrelevant background, and improve recognition performance under varying conditions like light, color, and intensity variations. Then, a region-based CNN with a RPN localizes disease regions. Finally, GRN after the fully connected layer refines the results for greater accuracy. The workflow is shown in Figure 2.

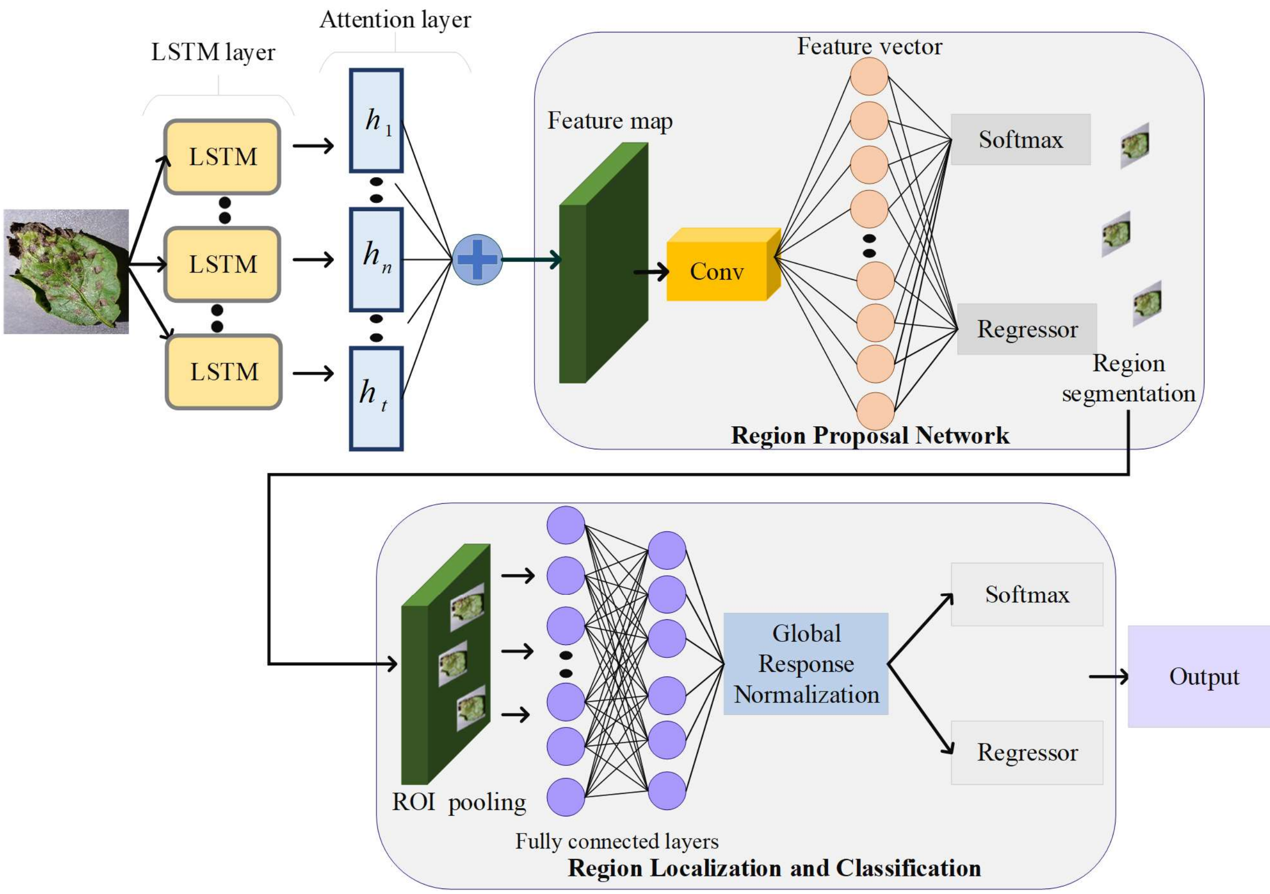

Figure 2: Design of proposed NLSCTAN model

LSTM with temporal attention model: After feature extraction, an LSTM model learns long temporal dependencies with input, output, and forget gates. The input gate, determining information to add to the cell state, uses a sigmoid layer to transform selected neurons and a Tanh layer to create a candidate vector $\left(\hat{C}_l\right)$, as represented in Equations (15-16),

$$i_l = \sigma\left(\omega_i.\left[h_{l-1}, y_l\right] + b_i\right) \tag{15}$$

$$\hat{C}_l = \tanh\left(\omega_c.\left[h_{l-1}, y_l\right] + b_c\right) \tag{16}$$

where i_l denotes the input gate activation, σ and tanh indicate the sigmoid and hyperbolic tangent activation function, respectively. y_l indicates the input, h_{l-1} denotes the hidden state from the previous time stamp. ω_i and ω_c specify the weight matrices for input and candidate gates respectively. b_i and b_c represent the bias matrices for input and candidate gates respectively.

The forget gate removes information from the cell state, updating it using a sigmoid layer with inputs and h_{l-1}. This mathematically represented in Equations (17-18),

$$f_l = \sigma\left(\omega_f .\left[h_{l-1}, y_l\right] + b_f\right) \tag{17}$$

$$C_l = f_l \Theta C_{l-1} + i_l \Theta \hat{C}_l \tag{18}$$

where Θ denotes the element wise multiplication, f_l denotes the forgot gate activation, C_l is the cell state, ω_f and b_f are the weight and bias for the forget gate, respectively. The output gate regulates the information passed to the next stage using a sigmoid layer and a tanh layer. The output gate (o_l) is computed using Equations (19-20),

$$o_l = \sigma\left(\omega_o .\left[h_{l-1}, y_l\right] + b_o\right) \tag{19}$$

$$h_l = o_l \Theta \tanh\left(C_l\right) \tag{20}$$

where h_l denotes the hidden state, ω_o and b_o are the weight and bias for the output gate, respectively. The LSTM model uses only the final hidden state, forgetting earlier information. Temporal attention in NLSCTAN incorporates all time steps, weighting important information. At each step (l), hidden states (h_l) are input, forming attention vector (S), with hidden states multiplied by attention weights (α_l). This is formulated in Equation (21),

$$S = \sum_{l=1}^{L} \alpha_l \times h_l \tag{21}$$

where L refers to the total number of time stamps, α_l denotes the attention weight for time step l. This structure extracts short- and long-term temporal features, enhancing feature expression and discriminability while suppressing useless temporal features using the temporal attention weight matrix.

Region proposal network: The RPN unit utilizes 3 × 3 convolutional layers to generate anchors and bounding boxes for object proposals. RPN plays a crucial role in identifying potential regions of interest within an image that may contain disease symptoms. It achieves this by generating bounding boxes around these regions, providing a localized focus for subsequent analysis.

ROI pooling: The ROI pooling layer combines features from convolutional layers and the RPN module to compute proposal feature maps for input to fully connected layers.

Global response normalization: To boost generalization, the model integrates GRN in the classification layer, enhancing channel contrast, selectivity, and addressing gradient issues for improved training convergence and model generalization.

Classification: The final step involves the classification module, which identifies diseased regions in potato crops by generating bounding boxes and determining categories.

Loss: The loss function comprises both classification and position regression losses, defined in Equation (22),

$$Loss(\{p_i\},\{s_i\}) = \sum_i Loss_{class}\left(p_i, p_i^*\right)/ N_{class} + \lambda \sum_i p_i * Loss_{regress}\left(s_i, s_i^*\right)/ N_{regress} \tag{22}$$

where i denotes the subscript of each sample, p_i denotes the probability of predicted class, p_i^* represents the ground truth label, s_i indicates the classified bounding box, and s_i^* denotes the ground truth. $Loss_{class}$ indicates the classification loss, $L_{regress}$ refers to the regression loss, N_{class} indicates the normalization term for the classification loss, $N_{regress}$ is the normalization factor for the normalization factor for the regression loss.

To minimize the loss function of the network, MWO algorithm is utilized. The MWO improves upon the original WO by incorporating the Lévy flight strategy, which allows broader search space exploration and enhances efficiency in finding optimal solutions. This metaheuristic approach improves convergence capabilities, making MWO [28] a powerful optimization tool. The flowchart in Figure 3 illustrates the MWO algorithm's optimization process.

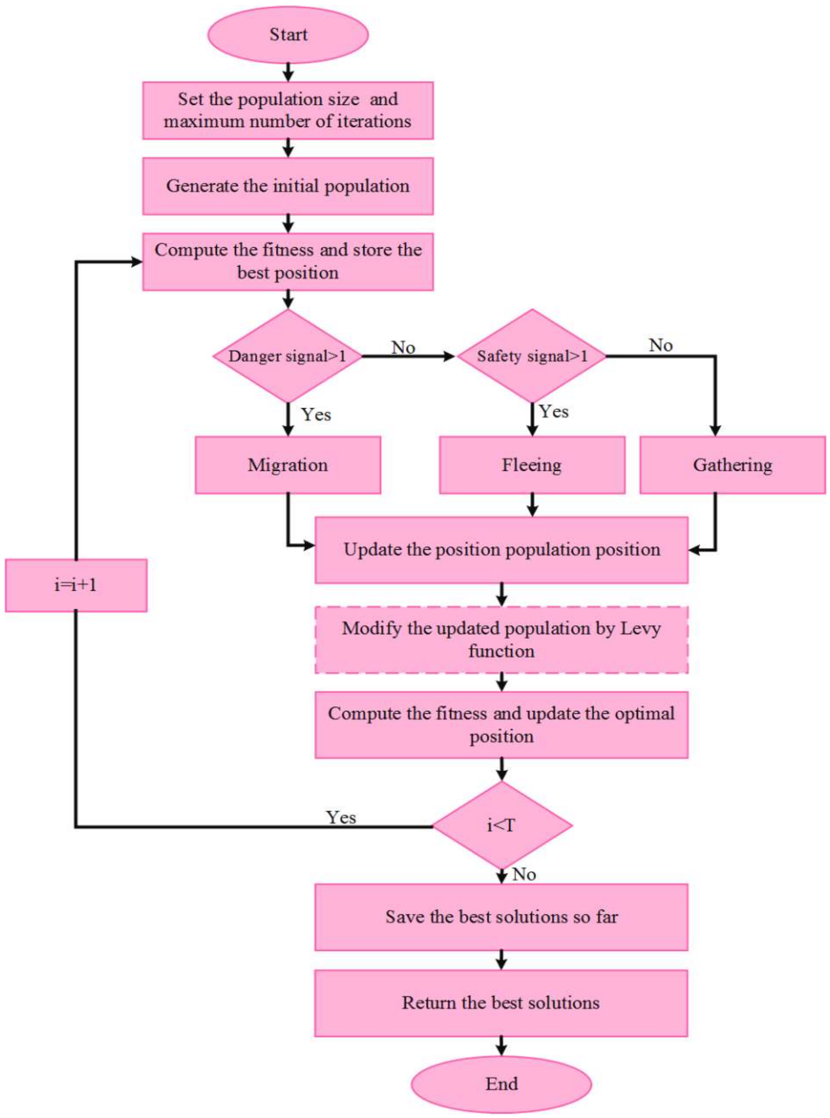

Figure 3: Flowchart of MWO algorithm

Initializing randomly generated solutions are optimized while adhering to the predefined range of variable boundaries. WO identifies the danger and safety signals that are vital in assessing walrus behavior, as shown in Equations (23 to 27) for the danger signal.

$$dngr\_sig = P \times S \tag{23}$$

$$P = 2 \times \beta \tag{24}$$

$$\beta = 1 - \frac{t}{T} \tag{25}$$

$$S = 2 \times r_1 - 1 \tag{26}$$

$$Saf\_sig = r_2 \tag{27}$$

where, P besides S highlights the danger factors, β falls between 1 and 0 during repetitions. r_1 and r_2 are the arbitrary variables lie between 0 and 1. r_2 defined as a safety signal. t indicates the repetition count, while T defines its maximum predetermined value. The walrus's position is recalculated based on parameters throughout the exploration phase. The position update is defined in Equations (28 to 30).

$$X_{ij}^{t+1} = X_{ij}^{t} + Mig\_step \tag{28}$$

$$Mig\_step = (X_u^t - X_v^t) \times \delta \times r_3^2 \tag{29}$$

$$\delta = 1 - \frac{1}{1 + e^{\frac{-10(t-0.5T)}{T}}} \tag{30}$$

where, X_{ij}^{t+1} denotes the updated position for the iteration i and dimension j. X_u^t and X_v^t are two arbitrarily chosen positions. Using the Halton sequence distribution, the male walrus positions are reassigned, while the female position is directed by both a male and the lead walrus, as detailed in Equations (31 to 34).

$$fem_{ij}^{t+1} = fem_{ij}^{t} + \beta \times (male_{ij}^{t} - fem_{ij}^{t}) + (1 - \beta) \times (X_{best}^{t} - fem_{ij}^{t}) \tag{31}$$

$$X_{best}^{t} = \sum_i Loss_{class}\left(p_i, p_i^*\right) / N_{class} + \lambda \sum_i p_i * Loss_{regress}\left(s_i, s_i^*\right) / N_{regress} \tag{32}$$

$$juv_{ij}^{t+1} = (Q - juv_{ij}^{t}) \times A \tag{33}$$

$$Q = X_{best}^{t} + juv_{ij}^{t} \times LF \tag{34}$$

where, Q represents the safety reference site, A Indicates the danger coefficient for juvenile walruses, with the vector representing LF Levy flight is based on Levy distribution that is the improvement of WOA. Therefore, the EWO achieves exceptional convergence performance, positioning it as a key tool for solving intricate optimization problems. The Levy function is presented in Equation (35).

$$LF = 0.01 \times \frac{m \times \sigma}{|n|^{\frac{1}{\gamma}}}, \sigma = \left(\frac{\Gamma(1+\gamma) \times \sin\left(\frac{\pi\gamma}{2}\right)}{\Gamma\left(\frac{1+\gamma}{2}\right) \times \gamma \times 2^{\left(\frac{\gamma-1}{2}\right)}} \right)^{\frac{1}{\gamma}} \tag{35}$$

The parameters m and n, being random variables range between 0 and 1. The suggested model identifies both healthy and diseased potato leaves while providing appropriate fertilizer recommendations.

This research work introduces a diverse dataset by combining similar classes from three distinct potato leaf datasets. Image quality is enhanced using adaptive CLAHE with double gamma correction preprocessing. Feature extraction involves extracting six texture features using TP-DWT, followed by dimensionality reduction with an AE. Disease segmentation-based classification utilizes a NLSCTAN for improved generalization and stability during training. MWO enhances accuracy by minimizing loss function, supporting timely disease detection and recommending suitable pesticides and fertilizers to increase potato crop yield.

4. Results and discussions

The following section details the findings of classifying potato leaf diseases with fertilizer suggestions using the proposed model, comparing with various existing methods. The proposed model is implemented on Python environment. Table 1 details the hyper parameters. Subsequent sections provide performance analysis for the NLSCTAN model.

Table 1: Hyper parameters setting of the proposed technique

Parameters	Values
Leaning rate	0.001
Maximum epochs	100

Batch size	32
Training algorithm	MWO
Kernel size	3

The introduced NLSCTAN scheme uses potato leaf images from the new dataset and performs pre-processing to eliminate noise, which may degrade system performance. This phase improves image quality before feature extraction. After pre-processing and feature extraction, the NLSCTAN handles detection and fertilizer suggestions. Simulation outcomes for potato leaf disease recognition are shown in Figure 4.

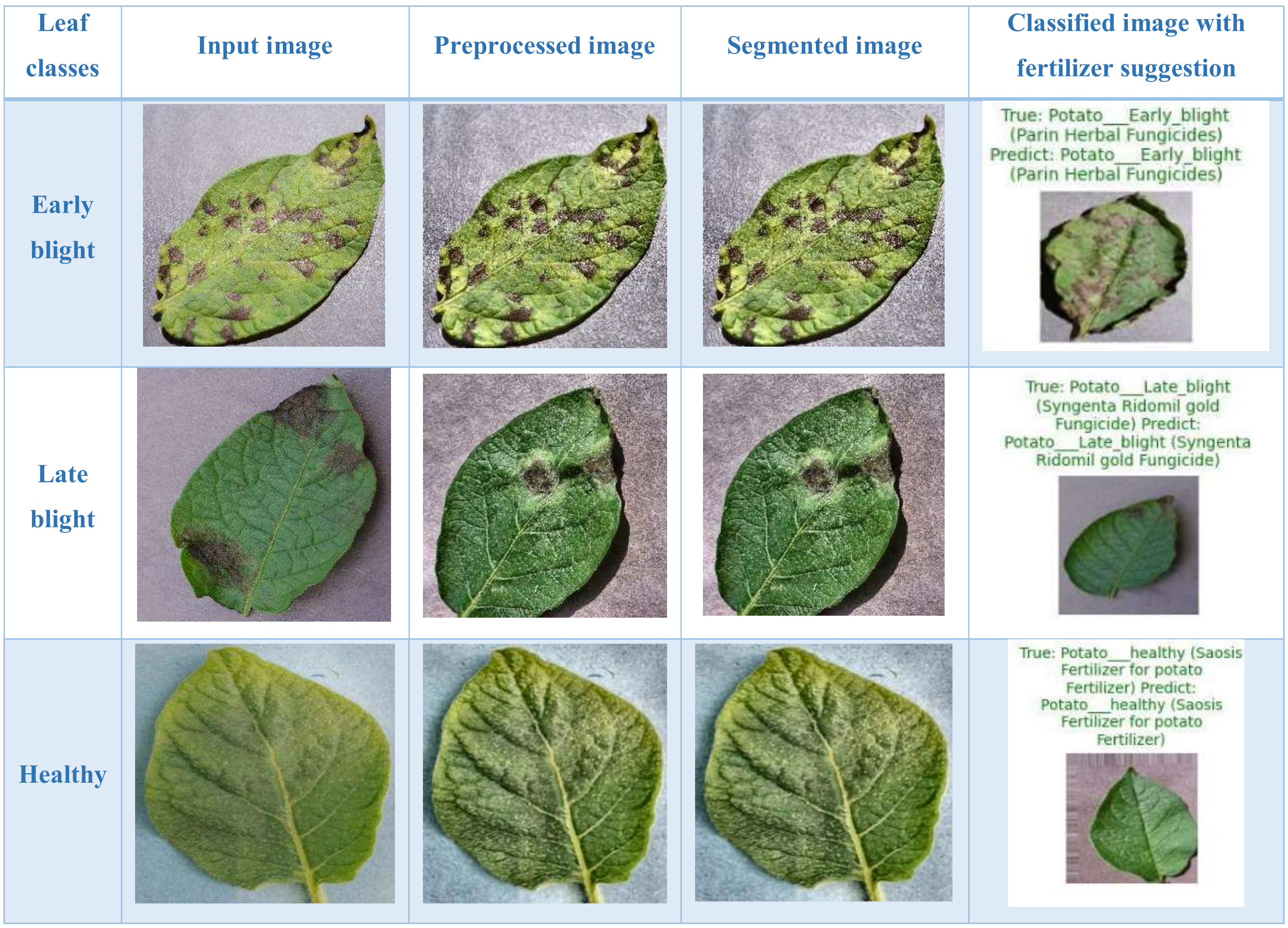

Figure 4: Outcomes of introduced NLSCTAN technique

4.1 Dataset description

A new dataset is constructed by combining similar classes from the potato leaf disease dataset [29], potato leaf diseases [30], and plant village dataset [16]. Each original dataset is randomly split into training, testing and validation sets (70:15:15) before being combined into a wide-ranging dataset. This comprehensive dataset includes the classes of healthy, late blight, and early blight from the three source datasets. Table 2 provides detailed information about the new dataset.

Table 2: Statistics of newly created dataset

Class names	Total (100%)	Train (70%)	Test (15%)	Validation (15%)
Early_Blight	3528	2470	529	529
Healthy	1472	1030	221	221
Light_Blight	2724	1908	408	408

The newly generated diverse dataset is stronger and more diverse than other datasets. For example, the plant village dataset, which originated from a collaborative project led by Penn State University, was created to support research in plant pathology and computer vision. Meanwhile, the potato leaf diseases dataset includes images collected from potato leaves in the Pakistani region. One significant advantage of this research work is the union of various datasets, which combines data with various sizes, shapes and backgrounds, and to generate a more comprehensive and larger dataset.

4.2 Performance analysis of introduced NLSCTAN scheme

The results of the introduced NLSCTAN technique for potato leaf disease recognition are presented in the subsection. The performance of the classification model is assessed across various parameters. Initially, optimal hyper parameters are determined, followed by a tuning process for improved results. After tuning, the best values selected include a learning rate of 0.001, 100 epochs, and the MWO optimizer algorithm. Furthermore, the model's performance is compared using different evaluation metrics to assess its progress.

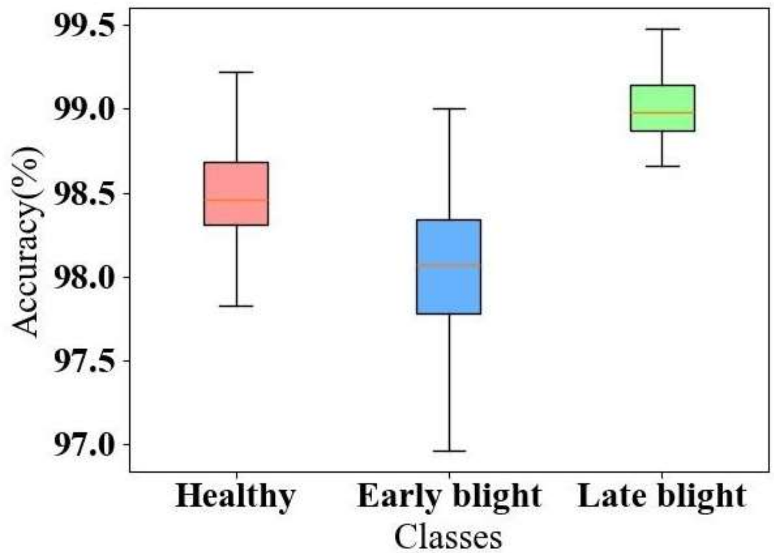

Figure 5: Graphical presentation of achieved accuracy results

The class-wise accuracy for three potato leaf groups is computed, and results are illustrated via box plots in Figure 5. Box plots depict maximum, mean, and minimum values, offering a comprehensive view of performance. Accuracy values in Figure 5 affirm the efficiency of the developed scheme in classifying infected potato leaves. Specifically, the proposed NLSCTAN technique achieves average accuracies of 98.5%, 98.4%, and 99.03% for healthy, early blight, and late blight classes, respectively.

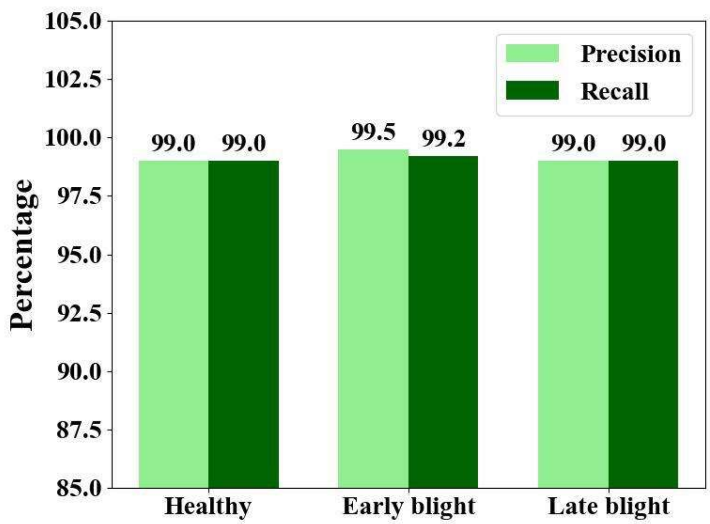

Figure 6: Visualization of the achieved precision and recall outcomes

The classification results are evaluated using recall and precision measures, standard for model classification assessment. Figure 6 displays achieved values for healthy, late blight, and early blight classes. The results indicate that the proposed approach effectively recognizes all three classes in the dataset. Recall values are 99%, 99%, and 99.2% for healthy, late blight, and early blight, respectively. Precision metrics yielded results of 99%, 99%, and 99.5% for the respective classes.

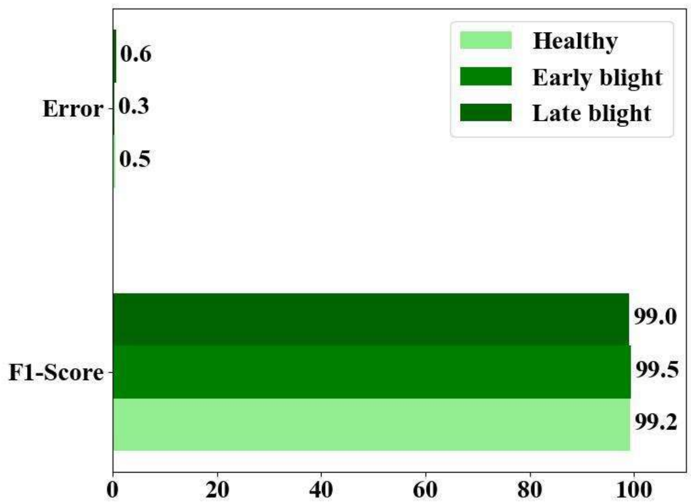

Figure 7: Visualization of achieved F1-score and Error rates

The proposed technique's performance is evaluated using F1-score and error rate metrics, providing a comprehensive assessment beyond precision and recall. This accounts for cases where maximizing precision or recall alone may not suffice. The method achieves a mean F1-score of 99.6%, as shown in Figure 7. Additionally, error rates range from 1.6% to 1.3%, indicating robust classification across all potato leaf disease classes.

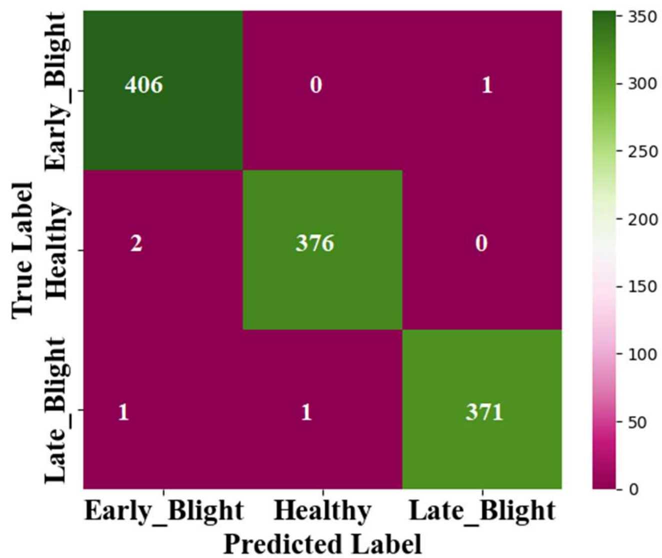

Figure 8: Achieved results using a confusion matrix

The class-wise performance of the approach is illustrated utilizing a confusion matrix, a powerful tool showcasing recognition ability based on true positive rates. Figure 9 depicts the confusion matrix for the strategy, revealing superior performance across all three potato leaf disease classes. The approach achieves an average true positive rate, indicating enhanced recall behavior.

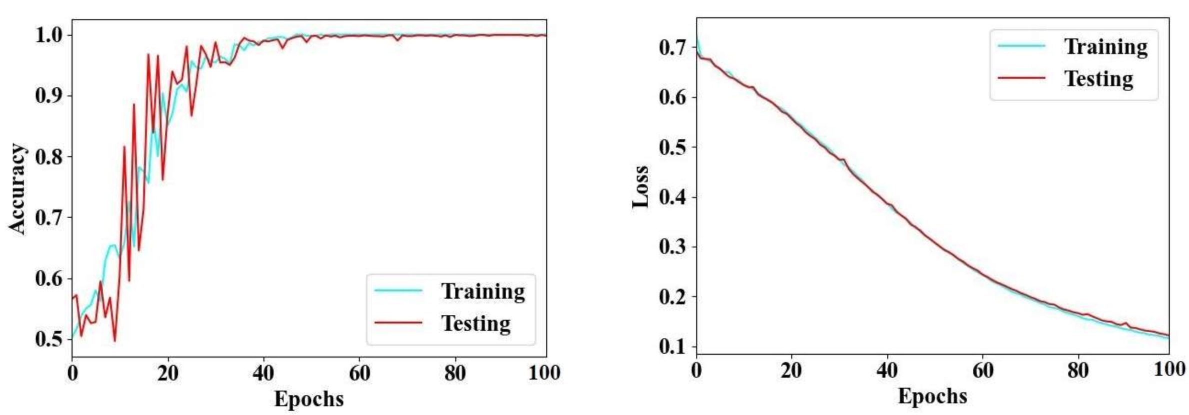

(a) (b)

Figure 9: Analysis of training and testing graphs (a) Accuracy (b) Loss

Figures 9a and 9b depict the accuracy and loss analysis of the proposed NLSCTAN technique during both training and testing phases. These graphs illustrate the accuracy and loss metrics of the potato leaf disease recognition model using NLSCTAN. By adjusting the epoch size, the classifier's accuracy and loss are evaluated throughout training and testing. NLSCTAN's accuracy improves during training at epoch 20, while loss decreases. Similarly, the model achieves maximum accuracy during testing, with reduced loss compared to training. The comparable training and testing curves demonstrate NLSCTAN's effectiveness in classifying potato leaf images, with superior outcomes observed. The error value indicates the gap between training and testing curves in disease detection, which diminishes with increased epochs, suggesting improved classification rates.

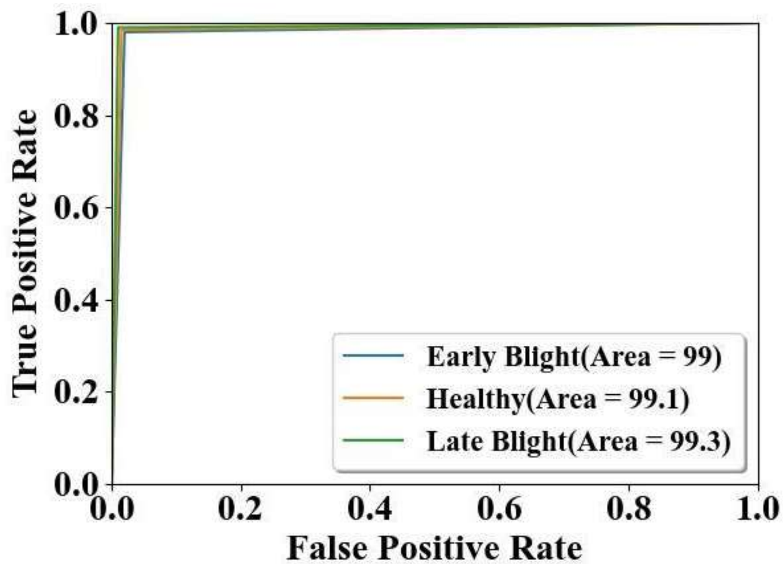

Figure 10: ROC analysis

The ROC analysis in Figure 10 showcases the classification model's ability to differentiate between various potato leaf conditions: early blight, healthy, and late blight. Higher Area Under the Curve (AUC) values denote better discriminative ability, with early blight at 0.99, healthy at 0.991, and late blight at 0.993. These values reflect strong classification performance, with late blight demonstrating the highest AUC, indicating excellent discrimination.

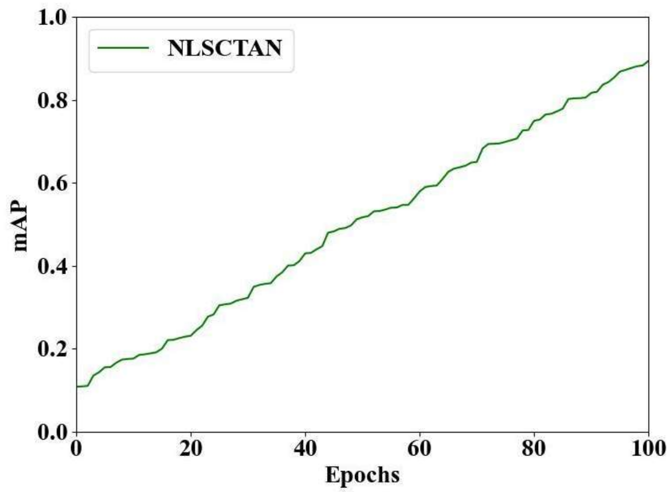

Figure 11: Mean average precision analysis

Figure 11 illustrates the mean Average Precision (mAP) values over 100 training epochs for the proposed model. Initially, the models show a steep increase in mAP, indicating rapid learning and improvement in precision during the early epochs. Over the remaining epochs, the proposed model maintains a mAP more than 0.8. This indicates that the model significantly enhances its precision in identifying the target classes.

4.3 Comparative analysis of the proposed NLSCTAN model

A comparative analysis is executed to confirm the efficacy of the introduced work compared to other approaches.

Table 3: Performance analysis of the proposed model with current models

Techniques	Accuracy (%)	Precision (%)	Specificity (%)	Recall (%)	F1-score (%)
MobS-Net [21]	97.33	-	98.39	91.99	91.99
Efficient PNet [31]	98.12	98.09	-	97.22	97.65
Efficient RMT-Net [32]	97.6	94.12	96	94	96.2
Ensemble model [20]	98.66	96.0	-	96.33	96.33

NLSCTAN (proposed)	99.2	99.7	99.8	99.4	99.6

Table 3 compares various techniques for potato leaf disease detection, including MobS-Net, Efficient PNet, Efficient RMT-Net, an Ensemble model, and the proposed NLSCTAN. The introduced NLSCTAN method reveals the highest performance across all metrics, with an accuracy of 99.2%, precision of 99.7%, specificity of 99.8%, recall of 99.4%, and F1-score of 99.6%. This indicates its capability to accurately detect and categorize potato leaf diseases. Furthermore, the proposed NLSCTAN benefits from its generalization ability, as it combines data with various sizes, backgrounds, and shapes, allowing for robust performance across different scenarios. Also, the proposed method minimizes the false negative rate, thereby improving the system's accuracy.

Table 4: Parameters analysis of the proposed scheme over recent models

Models	Parameters (million)	Accuracy (%)
Efficient PNet [31]	11	98.1
Improved YOLOv6s [33]	17.2	-
Scaled model +GRN+SE block [34]	19.07	99.2
Proposed NLSCTAN	0.066	99.2

Table 4 provides a comparison of DL architectures in terms of proposed model structure and performance, detailing total model parameters and accuracy. The proposed approach excels with 99.2% accuracy and 0.066 million model parameters, outperforming others. Its simplified model structure mitigates overfitting issues, making it an effective solution for identifying various potato plant leaf illnesses.

5. Conclusion

This research introduces a novel approach, designed to classify infected potato leaves and offer fertilizer recommendations to combat diseases. It leverages a diverse dataset obtained by amalgamating similar classes from three distinct potato leaf datasets. To enhance image quality, preprocessing involves adaptive CLAHE with double gamma correction. Feature extraction employs TP-DWT to extract various texture features, followed by dimensionality reduction through an AE. Subsequently, the NLSCTAN model, which combines DL-based semantic segmentation with classification abilities, is utilized to extract infected regions and identify them accurately. MWO further improves accuracy by minimizing the neural network's loss function. Experimental results show the proposed approach achieves 99.2% accuracy on a new diverse dataset, outperforming other models.

Future research will detect several diseases on a single leaf, estimate severity, localize diseases, develop an IoT-based monitoring scheme, and launch a mobile and website application. Based on the identified disease, the system suggests suitable pesticides for problems such as early blight and late blight. This guarantees precise treatments, promotes sustainability, and assists farmers in effectively managing potato crops.

Authors Contributions: All authors have contributed equally in data preparation, and analysis.

Data Availability Statement: All data generated or analyzed during this study are included in this published article.

Funding statement: Not applicable.

Informed consent: No human subjects are harmed in this research, and we confirmed that all data shared with the participants.

Conflict of Interest: Authors have no conflict of Interest.

References

1. Ali S, Hassan M, Kim JY, Farid MI, Sanaullah M, Mufti H. FF-PCA-LDA: intelligent feature fusion based PCA-LDA classification system for plant leaf diseases. Applied Sciences. 2022 Mar 30;12(7):3514.
2. Tarek H, Aly H, Eisa S, Abul-Soud M. Optimized deep learning algorithms for tomato leaf disease detection with hardware deployment. Electronics. 2022 Jan 3;11(1):140.
3. Lee TY, Lin IA, Yu JY, Yang JM, Chang YC. High efficiency disease detection for potato leaf with convolutional neural network. SN Computer Science. 2021 Jul;2(4):297.
4. Mahum R, Munir H, Mughal ZU, Awais M, Sher Khan F, Saqlain M, Mahamad S, Tlili I. A novel framework for potato leaf disease detection using an efficient deep learning model. Human and Ecological Risk Assessment: An International Journal. 2023 Feb 7;29(2):303-26.

5. Yeswanth PV, Khandelwal R, Deivalakshmi S. Super resolution-based leaf disease detection in potato plant using broad deep residual network (BDRN). SN Computer Science. 2022 Dec 20;4(2):112.
6. Hou C, Zhuang J, Tang Y, He Y, Miao A, Huang H, Luo S. Recognition of early blight and late blight diseases on potato leaves based on graph cut segmentation. Journal of Agriculture and Food Research. 2021 Sep 1;5:100154.
7. Kang F, Li J, Wang C, Wang F. A lightweight neural network-based method for identifying early-blight and late-blight leaves of potato. Applied Sciences. 2023 Jan 23;13(3):1487.
8. Al-Adhaileh MH, Verma A, Aldhyani TH, Koundal D. Potato blight detection using fine-tuned CNN architecture. Mathematics. 2023 Mar 21;11(6):1516.
9. Oishi Y, Habaragamuwa H, Zhang Y, Sugiura R, Asano K, Akai K, Shibata H, Fujimoto T. Automated abnormal potato plant detection system using deep learning models and portable video cameras. International Journal of Applied Earth Observation and Geoinformation. 2021 Dec 15;104:102509.
10. Dai G, Hu L, Fan J. DA-ActNN-YOLOV5: Hybrid YOLO v5 Model with Data Augmentation and Activation of Compression Mechanism for Potato Disease Identification. Computational Intelligence and Neuroscience. 2022;2022(1):6114061.
11. Hou B, Hu Y, Zhang P, Hou L. Potato late blight severity and epidemic period prediction based on vis/nir spectroscopy. Agriculture. 2022 Jun 21;12(7):897.
12. Sakkarvarthi G, Sathianesan GW, Murugan VS, Reddy AJ, Jayagopal P, Elsisi M. Detection and classification of tomato crop disease using convolutional neural network. Electronics. 2022 Nov 6;11(21):3618.
13. Wang J, Yu L, Yang J, Dong H. DBA_SSD: A novel end-to-end object detection algorithm applied to plant disease detection. Information. 2021 Nov 16;12(11):474.
14. Bedi P, Gole P. Plant disease detection using hybrid model based on convolutional autoencoder and convolutional neural network. Artificial Intelligence in Agriculture. 2021 Jan 1;5:90-101.
15. Kundu R, Dutta D, Nanda MK, Chakrabarty A. Near real time monitoring of potato late blight disease severity using field based hyperspectral observation. Smart Agricultural Technology. 2021 Dec 1;1:100019.

16. Elshewey AM, Tawfeek SM, Alhussan AA, Radwan M, Abed AH. Optimized Deep Learning for Potato Blight Detection Using the Waterwheel Plant Algorithm and Sine Cosine Algorithm. Potato Research. 2024 May 28:1-25.
17. Jha P, Dembla D, Dubey W. Deep learning models for enhancing potato leaf disease prediction: Implementation of transfer learning based stacking ensemble model. Multimedia Tools and Applications. 2024 Apr;83(13):37839-58.
18. Xu Y, Gao Z, Wang J, Zhou Y, Li J, Meng X. A Two-Stage Approach to the Study of Potato Disease Severity Classification. Agriculture. 2024 Feb 28;14(3):386.
19. Gupta HK, Shah HR. Deep Learning-Based Approach to Identify the Potato Leaf Disease and Help in Mitigation Using IOT. SN Computer Science. 2023 Apr 15;4(4):333.
20. Arshad F, Mateen M, Hayat S, Wardah M, Al-Huda Z, Gu YH, Al-antari MA. PLDPNet: End-to-end hybrid deep learning framework for potato leaf disease prediction. Alexandria Engineering Journal. 2023 Sep 1;78:406-18.
21. Chen J, Deng X, Wen Y, Chen W, Zeb A, Zhang D. Weakly-supervised learning method for the recognition of potato leaf diseases. Artificial Intelligence Review. 2023 Aug;56(8):7985-8002.
22. Feng J, Hou B, Yu C, Yang H, Wang C, Shi X, Hu Y. Research and Validation of Potato Late Blight Detection Method Based on Deep Learning. Agronomy. 2023 Jun 20;13(6):1659.
23. Kumar A, Patel VK. Classification and identification of disease in potato leaf using hierarchical based deep learning convolutional neural network. Multimedia Tools and Applications. 2023 Aug;82(20):31101-27.
24. Chen W, Chen J, Zeb A, Yang S, Zhang D. Mobile convolution neural network for the recognition of potato leaf disease images. Multimedia Tools and Applications. 2022 Jun;81(15):20797-816.
25. Chang Y, Jung C, Ke P, Song H, Hwang J. Automatic contrast-limited adaptive histogram equalization with dual gamma correction. Ieee Access. 2018 Jan 25;6:11782-92.
26. Tuncer T, Dogan S, Subasi A. Surface EMG signal classification using ternary pattern and discrete wavelet transform based feature extraction for hand movement recognition. Biomedical signal processing and control. 2020 Apr 1;58:101872.

27. Latif MA, Afshan N, Mushtaq Z, Khan NA, Irfan M, Nowakowski G, Alqhtani SM, Mursal S, Telenyk S. Enhanced classification of coffee leaf biotic stress by synergizing feature concatenation and dimensionality reduction. IEEE Access. 2023 Sep 12.
28. Alqahtani AH, Hasanien HM, Alharbi M, Chuanyu S. Parameters estimation of proton exchange membrane fuel cell model based on an improved Walrus optimization algorithm. IEEE Access. 2024 May 23.
29. Singh G, Yogi KK. Comparison of RSNET model with existing models for potato leaf disease detection. Biocatalysis and Agricultural Biotechnology. 2023 Jul 1;50:102726.
30. Rashid J, Khan I, Ali G, Almotiri SH, AlGhamdi MA, Masood K. Multi-level deep learning model for potato leaf disease recognition. Electronics. 2021 Aug 26;10(17):2064.
31. Nazir T, Iqbal MM, Jabbar S, Hussain A, Albathan M. EfficientPNet—An Optimized and Efficient Deep Learning Approach for Classifying Disease of Potato Plant Leaves. Agriculture. 2023 Apr 9;13(4):841.
32. Shaheed K, Qureshi I, Abbas F, Jabbar S, Abbas Q, Ahmad H, Sajid MZ. EfficientRMT-Net—An Efficient ResNet-50 and Vision Transformers Approach for Classifying Potato Plant Leaf Diseases. Sensors. 2023 Nov 30;23(23):9516.
33. Noon SK, Amjad M, Qureshi MA, Mannan A, Awan T. An Improved Detection Method for Crop & Fruit Leaf Disease under Real-Field Conditions. AgriEngineering. 2024 Feb 9;6(1):344-60.
34. Pacal I. Enhancing crop productivity and sustainability through disease identification in maize leaves: Exploiting a large dataset with an advanced vision transformer model. Expert Systems with Applications. 2024 Mar 15;238:122099.